JOURNAL OF PURE AND APPLIED MICROBIOLOGY, June 2015. Vol. **9**(2), p. 1149-1154

Numerical Analysis of Flow Patterns of Hydrogen-Sulfide inside Nasal Cavity

M.V. Shyla[1]*, K.B. Naidu[1], G. Vasanth Kumar[2] and Geetha Ramesh[3]

[1]Department of Mathematics, Sathyabama University, Chennai - 600 119, Tamil Nadu, India,
[2]Department of Aeronautical Engineering, Sathyabama University,
Chennai - 600 119, Tamil Nadu, India,
[3]Department of Anatomy and Histology, TANUVAS, Chennai - 600 051
Tamil Nadu, India.

(Received: 04 April 2015; accepted: 11 June 2015)

The objective of this paper is to explore flow patterns in nasal cavity . The nasal cavity of human and canine are considered in this study.The computational fluid dynamic (CFD) model of the nasal cavities are generated using CFD software Gambit and the analysis is done with Fluent software which employs finite volume method. The physical properties of hydrogen-sulfide are used in the CFD simulation. The flow patterns are visualized to understand implications of sensing.

Key words: Finite Volume Method, Human, Canine, Hydrogen-Sulfide, Nasal cavity.

Low levels of hydrogen-sulfide is present in the atmosphere. 4.5% to 45.5% is the explosive level of hydrogen-sulfide in air. Exposure to very high level can quickly lead to death. Increased concentration of hydrogen sulphide is possible in oil fields. Those living near waste water treatments, landfills and farms dealing with manure storage are also exposed to high levels of hydrogen-sulfide[1-2]

This study aims to discuss flow patterns of hydrogen-sulfide inhaled by human and canine using CFD. The nasal cavity is designed for both functions namely chemical sensing and respiratory air conditioning. But the process of olfaction and respiration takes place with a different flow path through the nasal cavity. Many researchers have analyzed airflow patterns in the nasal cavities in vitro using cast molds. The dynamic flow patterns can be understood with the help of Computational Fluid Dynamics (CFD) . It is also less expensive in comparison with experimental study[3-9]

* To whom all correspondence should be addressed.
E-mail: shylamv@yahoo.com

MATERIALS AND METHODS

The geometry of human nasal cavity is developed with the help of CT scan obtained from Bharat Scans, Chennai, India. To investigate the flow pattern in dog, geometry is obtained from the medical illustations[10]

The results of this study helps to observe the flow pattern of hydrogen-sulfide inside human and canine nasal cavity and can be used for designing artificial noses . Velocity is given as the inlet condition. Velocity is closely related to pressure, and density as seen in equations (1), (2) and (3). End results in terms of velocity can be easily converted to pressure, and density. Hence this method is advantageous over other methods.

The paper highlights the mathematical formulation, methodology, results and discussion

followed by validation of our results and conclusion.

Mathematical Formulation

Navier-Stokes system of equations for a two dimensional, unsteady, incompressible flow namely,

Equation of continuity: $\frac{\partial \rho}{\partial t} + \nabla.(\rho \vec{q}) = 0$ ...(1)

x-momentum equation:

$$\left(\frac{\partial(\rho u)}{\partial t} + \nabla.(\rho u \vec{q})\right) = -\frac{\partial p}{\partial x} + \nabla.(\mu \nabla u)$$ ...(2)

y-momentum equation:

$$\left(\frac{\partial(\rho v)}{\partial t} + \nabla.(\rho v \vec{q})\right) = -\frac{\partial p}{\partial y} + \nabla.(\mu \nabla v)$$ ...(3)

$\vec{q} = u\vec{i} + v\vec{j}$ is the velocity vector where u and v are the velocity components in the x and y directions respectively, p is pressure, ñ is density, μ is coefficient of viscosity, and t is time. All body forces are ignored.

An unsteady, viscous, incompressible flow inside human nasal cavity and canine nasal cavity is simulated with hydrogen-sulfide under laminar flow conditions. An uniform velocity of 1m/s is applied at the inlet in the case of canine sniffing and 0.1m/s is applied at the inlet of human nostril to induce the flow. The walls are taken as rigid. No slip boundary condition on the velocity is assumed at the walls. The physical properties of hydrogen-sulfide are taken for analysis. The density and coefficient of viscosity of hydrogen-sulfide are ρ=1.46kg/m3 and μ=1.2e-05 kg/m-s.

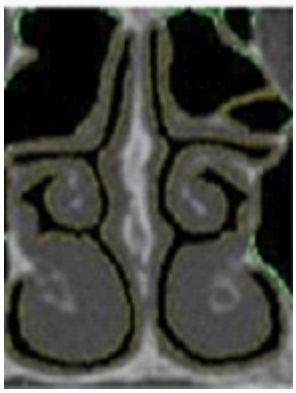

Fig.1. Human Nasal Cavity generated using Mimics Software

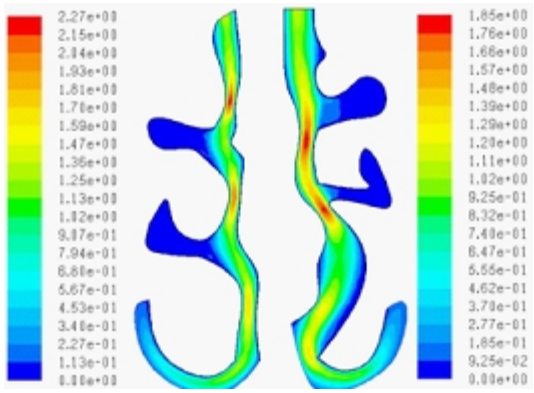

Fig. 2a. Velocity profile inside human nasal cavity

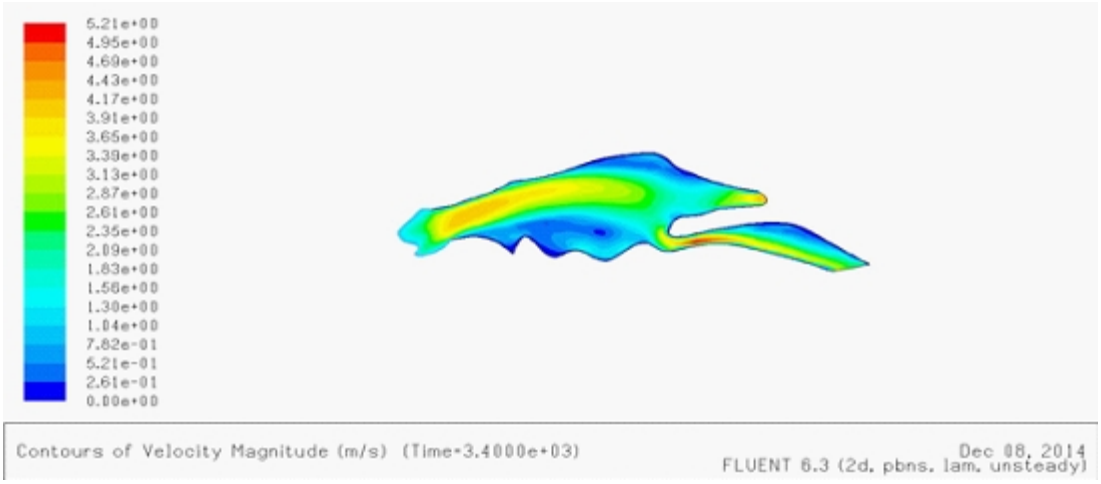

Fig. 2b. Velocity Profile inside dog's nasal cavity

Methodology

The CT image of the subject was loaded in MIMICS 10 software. MIMICS displays image in three different views namely the coronal view, axial view, and sagittal view. The coronal view best illustrates the nasal structure as shown in Fig.1. Different segmentation techniques like threshold, region growing, and crop masking are applied. The nasal geometry of human nose taken from mimics is fed into Gambit software using which a computational volume is created. The geometry of dog's nasal cavity in saggital view is considered in this study . The length of the nasal cavity from the nostril to the olfactory slit is taken around 9cm.

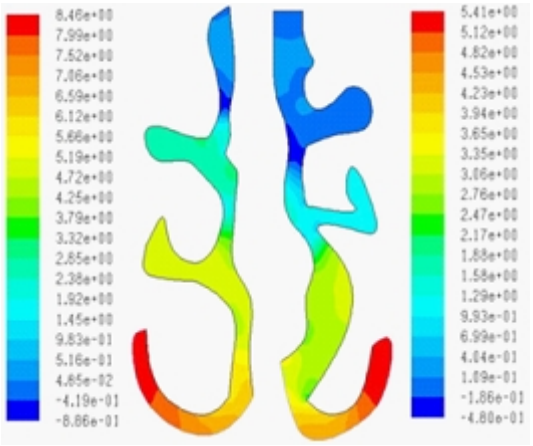

Fig. 3a. Pressure Distribution inside human nasal cavity

The problem is solved in three steps namely discretization, analysis and post processing of the results. The quadrilateral pave mesh is generated for the entire domain under consideration. The number of nodes and quadrilateral cells is obtained by fixing the interval size as 0.25 for each CFD model. There are 1633 nodes and 1406 quadrilateral cells in right nasal cavity of human, 1887 nodes and 1666 quadrilateral cells in left nasal cavity of human. In the case of dog there are 1972 nodes and 1812 quadrilateral cells.The boundaries inlet, outlet and the wall are defined for all CFD models.

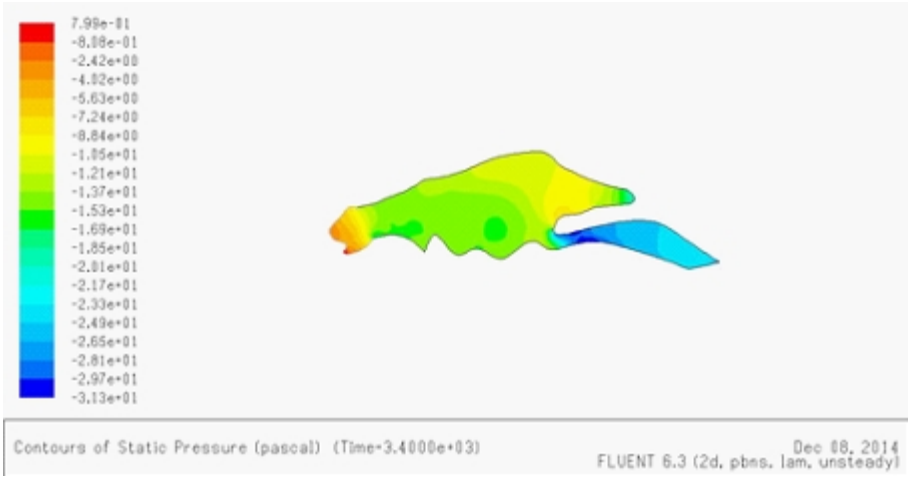

Fig. 3b. Pressure Distribution inside dog's nasal cavity

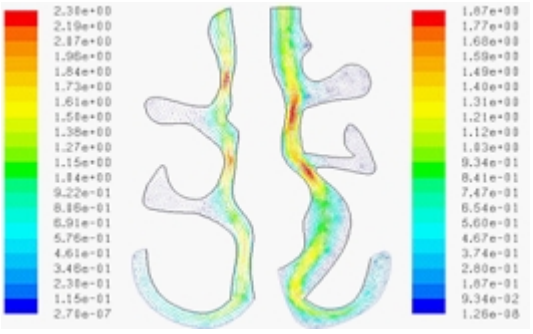

Fig. 4a. Streamline pattern inside human nasal cavity

The governing differential equations system is discretized over each control volume by upwind differencing scheme and is converted to algebraic system of equations which are solved iteratively by segregated solver using Semi-Implicit Method for Pressure Linked Equations popularly known as SIMPLE algorithm. Convergence of the solution correct to three decimal places is checked. 500 iterations are performed .

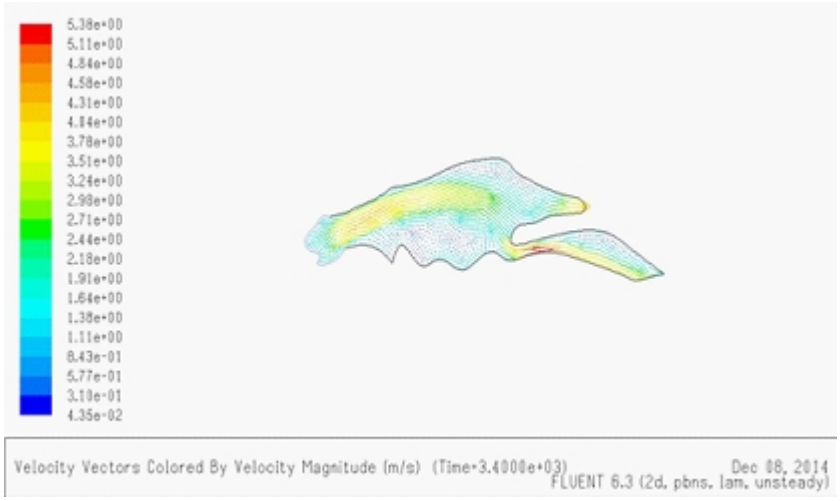

Fig. 4b. Streamline pattern inside dog's nasal cavity

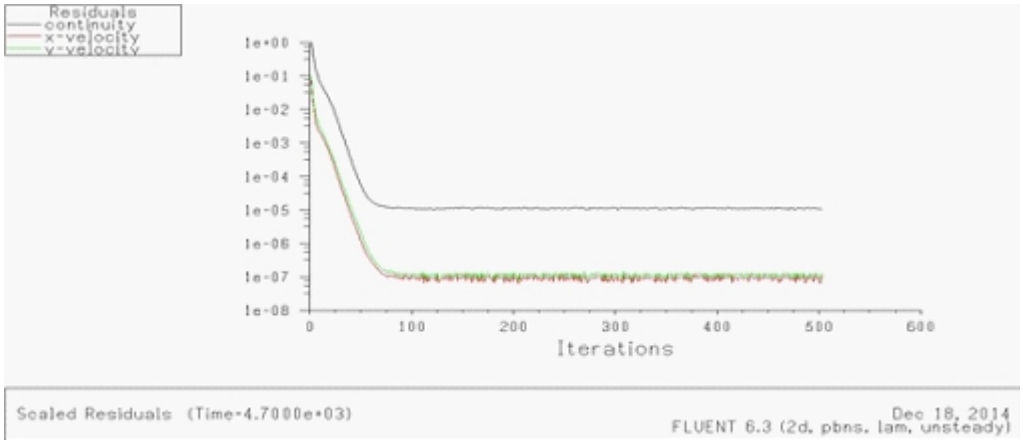

Fig. 5a. Velocity iteration plot-human-left

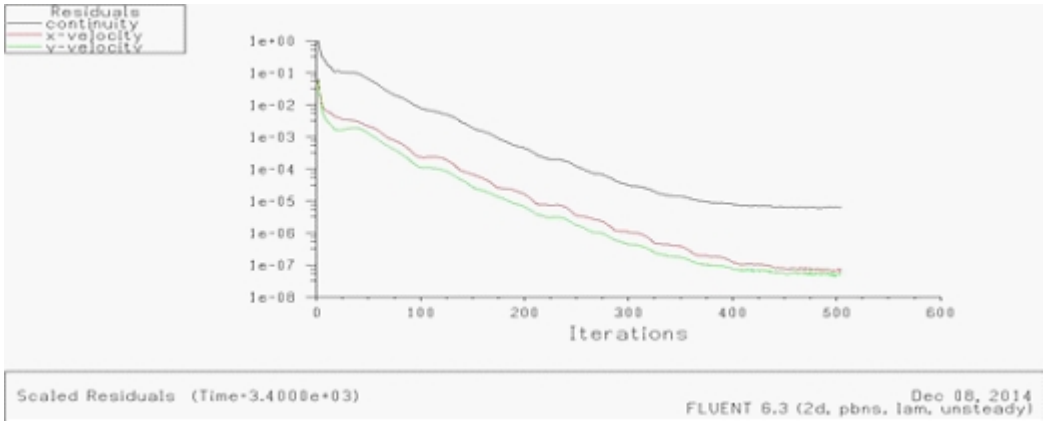

Fig. 5b. Velocity iteration plot-dog

Structured mesh is applied. Grid validation is also done. Perfect mesh combination is achieved to identify the flow pattern by changing the number of nodes and shape of the mesh. Convergence of the solution correct to three decimal places is monitored.

Analysis of Results

Air and the odorant in the immediate vicinity of the nostril towards the naris(inlet), inducing flow inside the nasal cavity. The flow pattern of hydrogen-sulfide inside human and canine nasal cavity can be visualized from Fig.2a and Fig.2b. The velocity magnitude at various points of nasal cavity can be viewed with the help of different contours as seen in Fig.2a and Fig.2b. Blue contour denotes very low velocity and red contour represents very high velocity.

High velocity(red contour) is observed in the middle airway. As the fluid reaches the olfactory slit the magnitude of velocity decreases Very low velocity(blue contour) is found in the nasal meatuses.The velocity magnitude near the olfactory slit is 0.79m/s in the left nasal cavity and 0.74 in the right nasal cavity. In this study, it is observed that the fluid flows with high velocity along the dorsal airway and as fluid reaches the olfactory region there is a decrease in velocity which is an implication of sensing.The magnitude of velocity near the olfactory region is 2.35m/s. Part of the air flow through the olfactory slit (upper end) into the olfactory region for olfaction and part of the air flows into the nasopharynx(lower end) for respiration which explains the multipurpose functioning of nose.

Pressure at the inlet is very high when compared to other points in human and dog nasal cavity. But as the fluid flows there is a pressure drop. In this case study of human the pressure drop is more in the case of right nasal cavity. The pressure distribution at different points of the nasal cavity is presented in Fig.3a and Fig.3b.

Streamline pattern given in Fig.4a and Fig.4b depicts the pattern of flow of fluid particles. Convergence of the Solution correct to 3 decimal places is monitored and is presented in Fig.5a and Fig.5b. The solution converges at 35th iteration for human left nasal cavity, 53rd iteration for human right nasal cavity, and 173rd iteration in the case of dog.

CONCLUSION

The results of this analysis can be used in the design of artificial noses and bio-inspired sensors .The design can target a particular industry based on the need. This study can be extended to perform biomimicry to derive efficient sniffing schemes in the artificial sensors. Single and multiple flows of different toxic chemicals can be considered under various boundary conditions using CFD analysis. The geometry can be customized to suit a particular industry.

ACKNOWLEDGMENTS

Our sincere thanks to Veterinary college and Bharat scans, Chennai, India for providing geometry of dog nasal cavity and human CT scan data.

REFERENCES

1. Hydrogen-Sulfide http://en.wikipedia.org/wiki/Hydrogen_sulfide
2. Hydrogen-Sulfide leak in siam-square http://bangkok.coconuts.co/2014/10/21/do-not-breathe-dangerous-toxic-gas-found-siam-square-one
3. Clement, P.A., Gordts, F. Standardisation Committee on Objective Assessment of the Nasal Airway IRS and ERS (2005) Consensus report on acoustic rhinometry and rhinomanometry. *Rhinology*, 2005; **43**(3): 169–179.
4. Craven, B.A., Paterson, E.G., Settles, G.S. The Fluid Dynamics of Canine Olfaction: Unique Nasal Airflow patterns as an Explanation of Macrosmia. *Journal of Royal Society Interface*, 2010; **7**(47): 933-943.
5. Craven, B.A., Paterson, E.G., Settles, G.S. Development and Verification of a High- Fidelity Computational Fluid Dynamics Model of Canine Nasal Airflow. *Journal of Biomechanical Engineering*, 2009; **131**: 1-11.
6. Hahn, I., Scherer, P.W., Mozell, M.M. A mass transport model of olfaction. *Journal of Theoretical Biology*, 1994; **167**(2): 115–128.
7. Lawson, M.J., Craven, B.A., Paterson, E.G., Settles, G.S. A Computational Study of Odorant Transport and Deposition in the Canine Nasal Cavity: Implications for Olfaction. *Oxford Journals Chemical Senses*, 2012; **37**(6): 553-566.

8. Settles, G.S. Sniffers: Fluid –Dynamic Sampling for Olfactory Trace Detection in Nature and Homeland Security-the 2004 Freeman Scholar Lecture. *Journal of Fluids Engineering*, 2005; **127**(2) : 189-218.
9. Shyla, M.V., Naidu, K.B. A Computational Fluid Dynamic Model of Human Sniffing. *Journal of Mathematical Science and Engineering*, 2013; **7**(1): 1243-1247.
10. Yesko, J. Medical Illustration of Canine Nasal Cavity. 1990. Available at : http://www.yesko.com/medical.../stock-illustration-dog-anatomy-03.htm